

Oxygen-Containing Functional Groups on Single-Wall Carbon Nanotubes: NEXAFS and Vibrational Spectroscopic Studies

Anya Kuznetsova,[†] Irene Popova,[†] John T. Yates, Jr.,^{*,†} Michael J. Bronikowski,^{*,§} Chad B. Huffman,[‡] Jie Liu,^{||} Richard E. Smalley,[‡] Henry H. Hwu,[⊥] and Jingguang G. Chen^{*,†}

Contribution from the Department of Chemistry, Surface Science Center, University of Pittsburgh, Pittsburgh, Pennsylvania 15260, Department of Chemistry, Rice University, Houston, Texas 77005, and Department of Materials Science, and Engineering, University of Delaware, Newark, Delaware 19716

Received April 23, 2001

Abstract: Single-walled nanotubes (SWNTs) produced by plasma laser vaporization (PLV) and containing oxidized surface functional groups have been studied for the first time with NEXAFS. Comparisons are made to SWNTs made by catalytic synthesis over Fe particles in high-pressure CO, called HiPco material. The results indicate that the acid purification and cutting of single-walled nanotubes with either HNO₃/H₂SO₄ or H₂O₂/H₂SO₄ mixtures produces the oxidized groups (O/C = 5.5–6.7%), which exhibit both $\pi^*(\text{CO})$ and $\sigma^*(\text{CO})$ C K-edge NEXAFS resonances. This indicates that both carbonyl (C=O) and ether C–O–C functionalities are present. Upon heating in a vacuum to 500–600 K, the $\pi^*(\text{CO})$ resonances are observed to decrease in intensity; on heating to 1073 K, the $\sigma^*(\text{CO})$ resonances disappear as the C–O–C functional groups are decomposed. Raman spectral measurements indicate that the basic tubular structure of the SWNTs is not perturbed by heating to 1073 K, based on the invariance of the ring breathing modes upon heating. The NEXAFS studies agree well with infrared studies which show that carboxylic acid groups are thermally destroyed first, followed by the more difficult destruction of ether and quinone groups. Single-walled nanotubes produced by the HiPco process, and not treated with oxidizing acids, exhibit an O/C ratio of 1.9% and do not exhibit either $\pi^*(\text{CO})$ or $\sigma^*(\text{CO})$ resonances at the detection limit of NEXAFS. It is shown that heating (to 1073 K) of the PLV-SWNTs containing the functional groups produces C K-edge NEXAFS spectra very similar to those seen for the HiPco material. The NEXAFS spectra are calibrated against spectra measured for a number of fused-ring aromatic hydrocarbon molecules containing various types of oxidized functional groups present on the oxidized SWNTs.

I. Introduction

A. Studies of Oxidized Carbon Nanotubes. Carbon nanotubes, seamlessly rolled-up graphene sheets of carbon, are one of the most promising molecular structures for a wide range of future technological innovations. They are expected to find numerous applications as for example: containers for molecules, salts, and metals; biological and chemical sensors; filled carbon nanotubes, used for magnetic recording; nanoelectronic devices; tips for scanning probe microscopy; flat panel displays; composite materials, etc.¹ An oxidative acid treatment is often used for nanotube purification. As a result of oxidizing acid attack, the ends and surfaces of nanotubes become covered with oxygen-containing groups such as carboxylate groups, ether groups, etc.² The presence of oxygenated groups on nanotubes is important both for nanotube application in electronic devices³ and as gas storage media.⁴ These oxygenated groups block entry

ports at the nanotube ends and at vacancy defect sites on nanotube walls and retard adsorption. For example, we determined earlier that the adsorption capacity of single-wall carbon nanotubes and the rate of adsorption of xenon at 95 K increased dramatically when nanotubes are activated by heating to 1073 K.⁵ During this thermal treatment CO, CO₂, CH₄, and H₂ are evolved. Infrared studies showed the existence of carboxylic, quinone, and ether groups on acid-purified nanotube samples before thermal treatment² and detected the removal of many of these groups by heating.

The importance of oxygenated groups on nanotube surfaces was also confirmed by the study of the oxidation of single-wall nanotube surfaces using ozone at 300 K.⁶ The ozone reaction with carbon nanotubes results in the formation of oxygenated groups without the destruction of the tubular structure of the carbon nanotubes. A reactive defect level involving ~5.5% of the carbon atoms in the nanotube sample was measured by reaction with ozone.⁶

[†] University of Pittsburgh.

[‡] Rice University.

[§] Present address: Jet Propulsion Laboratory, Pasadena, CA 91109.

^{||} Present address: Department of Chemistry, Duke University, Durham, NC 27708.

[⊥] University of Delaware.

(1) Harris, P. J. F. *Carbon Nanotubes and Related Structures*; Cambridge University Press: Cambridge, U.K., 1999. Dresselhaus, M. S.; Dresselhaus, G.; Eklund, P. C. *Science of Fullerenes and Carbon Nanotubes*; Academic Press: San Diego, CA, 1996.

(2) Kuznetsova, A.; Mawhinney, D. B.; Naumenko, V.; Yates, J. T., Jr.; Liu, J.; Smalley, R. E. *Chem. Phys. Lett.* **2000**, *321*, 292.

(3) Rochefort A.; Avouris P. *J. Phys. Chem. A* **2000**, *104*, 9807.

(4) Maniwa Y.; Kumazawa Y.; Saito Y.; Tou H.; Kataura H.; Ishii H.; Suzuki S.; Achiba Y.; Fujiwara A.; Suematsu H. *Mol. Cryst. Liq. Cryst.* **2000**, *340*, 671.

(5) Kuznetsova, A.; Yates, J. T., Jr.; Liu, J.; Smalley, R. E. *J. Chem. Phys.* **2000**, *112*, 9590.

(6) (a) Mawhinney, D. B.; Naumenko, V.; Kuznetsova, A.; Yates, J. T., Jr.; Liu, J.; Smalley, R. E. *J. Am. Chem. Soc.* **2000**, *122*, 2383. (b) Mawhinney, D. B.; Naumenko, V.; Kuznetsova, A.; Yates, J. T., Jr.; Liu, J.; Smalley, R. E. *Chem. Phys. Lett.* **2000**, *324*, 213.

B. Near-Edge X-ray Absorption Fine Structure (NEXAFS). NEXAFS provides electronic and structural information about atoms, molecules, and local chemical functionalities.

In a NEXAFS experiment, a tunable monochromatized high flux of X-ray photons (10^{13} – 10^{14} photons/s \cdot mm 2 \cdot mr $^{-2}$ \cdot (0.1% bandwidth) $^{-1}$ 7 excites an electron from an atomic core level to empty or partially occupied valence electronic states. 8 At photon energies in resonance with these transitions, a large increase in excitation cross section is observed. A subsequent electronic deexcitation process causes the emission of Auger electrons and fluorescence photons. The emission of electrons contributes to an increased electron yield indicative of the photon resonance for excitation to the higher energy states. Based on the kinetic energy, the electron yield measurements in NEXAFS can be performed in three modes: Auger electron yield (AEY), partial electron yield (PEY), and total electron yield (TEY). One of the main differences among these three methods of measuring the yield is the bulk and surface sensitivity of each. The PEY method is employed by us in the current work. For this method, the energy of the registered electrons is set to some threshold E_a ($E_a = 100$ eV) by negatively biasing the entrance of the detector to eliminate photoelectrons, originating from deep within the bulk. The large portion of emitted electrons come from the Auger transitions, which have an escape depth of ~ 10 Å.

C. “Building Blocks” NEXAFS Approach for Large Molecules. For large organic molecules, a “building blocks” approach 8 is used to interpret the NEXAFS measurements. In a simple picture, the NEXAFS spectra of these large molecules are a superposition of spectra from smaller fragments. Thus, different molecules containing carboxylate groups ($-\text{CO}_2^-$) were studied using NEXAFS. Each of the C K-edge spectra showed three peaks that are characteristic of the carboxylate group. The peak at approximately 288–289 eV is a sharp C=O π^* resonance, the peak at 296 eV is a σ^* resonance, and the peak at 302 eV is a C=O σ^* resonance. Both the gas-phase inner-shell electron energy loss spectra (ISEELS) of formic acid and methyl formate and the NEXAFS spectrum of poly(methyl methacrylate) show these “fingerprint” peaks for carboxylate groups. 8 – 11

A C K-edge NEXAFS study was also performed on polymerized C_{60} molecules. 12 In a similar, building blocks approach, the main resonances of pristine C_{60} are also observed in a cross-linked 2D structure of C_{60} molecules, including both the π^* (284–290 eV) and σ^* (292–303 eV) structure. 12 The building blocks approach also works well on unconjugated systems, when the localized nature of NEXAFS excitation is retained. 8

NEXAFS studies have been reported of the electronic structure of smaller fullerenes, such as C_{60} – C_{96} , 13,14 their fluorinated derivatives, 15 and nanostructural carbon. 16 To the best of our knowledge, this is the first report of NEXAFS spectra of single-wall carbon nanotubes.

(7) Vaughan, D. Ed. *X-ray Data Booklet*; Lawrence Berkeley Laboratory: University of California, 1986.

(8) Stöhr, J. *NEXAFS Spectroscopy*; Springer-Verlag: Berlin, 1992.

(9) Ishii, I.; Hitchcock, A. P. *J. Chem. Phys.* **1987**, *87*, 830.

(10) Ishii, I.; Hitchcock, A. P. *J. Electron. Spectrosc.* **1988**, *46*, 55.

(11) Outka, D. A.; Stöhr, J. In *Chemistry and Physics of Solid Surfaces*; Vanselow, V. R., Howe, R., Eds.; Springer Series in Surface Sciences VII; Springer: Berlin, 1988; Vol. 10, p 201.

(12) Schulte, J.; Böhm, M. C.; Schedel-Niedrig, T.; Schlögl, R. *Ber. Bunsen-Ges. Phys. Chem.* **1997**, *101*, 1531.

(13) Terminello, L. J.; Shuh, D. K.; Himpfel, F. J.; Lapiano-Smith, D. A.; Stöhr, J.; Bethune, D. S.; Meijer, G. *Chem. Phys. Lett.* **1991**, *182*, 491.

(14) Mitsumoto, R.; Oji, H.; Mori, I.; Yamamoto, Y.; Asato, K.; Ouchi, Y.; Shinohara, H.; Seki, K.; Umishita, K.; Hino, S.; Nagase, S.; Kikuchi, K.; Achiba, Y. *J. Phys. IV Fr.* **1997**, *7*, C2–525.

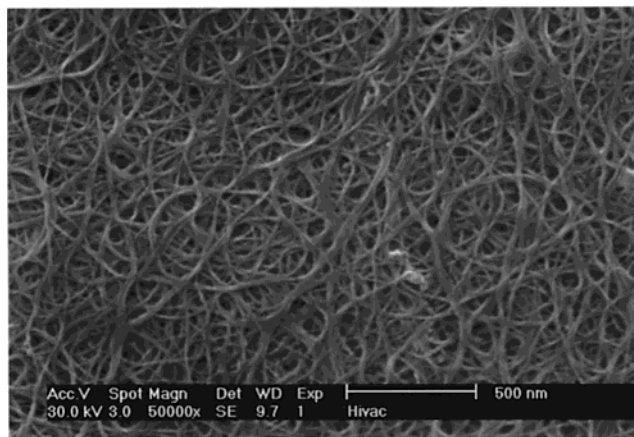


Figure 1. SEM image of carbon nanotubes produced by the pulsed-laser vaporization method.

In this study, we report the C K-edge and O K-edge NEXAFS studies of single-wall carbon nanotubes. The carbon nanotubes studied here are produced (1) by pulsed laser vaporization (PLV) followed by oxidizing acid purification and cutting and (2) by the gas-phase chemical vapor deposition (CVD) technique, which uses CO and metal carbonyls, and is called the HiPco process. Several organic compounds containing a variety of organic functional groups were compared to the measured NEXAFS spectra of nanotubes, serving as references to the spectral assignment.

II. Experimental Section

A. Preparation of Carbon Nanotube Samples. Four samples of single-wall carbon nanotubes were prepared by the pulsed laser vaporization technique (PLV). 17 The raw tubes were purified in an HNO_3 solution followed by treatment in a solution of $\text{HNO}_3/\text{H}_2\text{SO}_4$. The single-walled nanotubes (SWNTs) prepared by this technique are believed to have closed ends and are designated as c-SWNTs. The purified material was also cut using sonication in an $\text{H}_2\text{O}_2/\text{H}_2\text{SO}_4$ solution. 17 These tubes are referred to as o-SWNTs (open tubes). The samples of nanotubes (c-SWNT or o-SWNT) were suspended in methanol and deposited onto a Au-covered Ta foil using a drop/dry technique.

One sample of carbon nanotubes was prepared using catalytic clusters of iron in a high pressure of flowing CO (30–50 atm) (HiPco process 18). Catalytic Fe clusters are formed in situ, when Fe is added to the gas flow in the form of $\text{Fe}(\text{CO})_5$. The raw HiPco tubes are characterized as having 97% purity. 18 The samples of HiPco nanotubes were pressed onto a tungsten grid containing 0.2-mm-wide square holes.

Both the Au-covered Ta foil holder and the W-grid holder were mounted onto the manipulator, using two interlock holders, described previously. 5,19

B. Characterization of Carbon Nanotubes. The nanotubes were characterized using SEM and Raman spectroscopy.

The SEM images of both PLV and HiPco carbon nanotubes are shown in Figure 1 and Figure 2. To investigate the possibility of a structural change of the nanotubes due to exposure to a high flux of

(15) Mitsumoto, R.; Seki, K.; Araki, T.; Ito, E.; Ouchi, Y.; Achiba, Y.; Kikuchi, K.; Yajima, S.; Kawasaki, S.; Okino, F.; Touhara, H.; Kurosaki, H.; Sonoda, T.; Kobayashi, H. *J. Electron Spectrosc. Relat. Phenom.* **1996**, *78*, 453.

(16) Hwu, H. H.; Subramoney, S.; Foley, H. C.; Chen, J. G., unpublished results.

(17) Liu, J.; Rinzler, A. G.; Dai, H. J.; Hafner, J. H.; Bradley, R. K.; Boul, P. J.; Lu, A.; Iverson, T.; Shelimov, K.; Huffman, C. B.; Rodriguez-Macias, F.; Shon, Y.-S.; Lee, T. R.; Colbert, D. T.; Smalley, R. E. *Science* **1998**, *280*, 1253.

(18) Bronikowski, M.; Willis, P. A.; Colbert, D.; Smith, K. A.; Smalley, R. E., submitted to JVST.

(19) Yates, J. T., Jr. *Experimental Innovations in Surface Science*; Springer: New York, 1998; p 100.

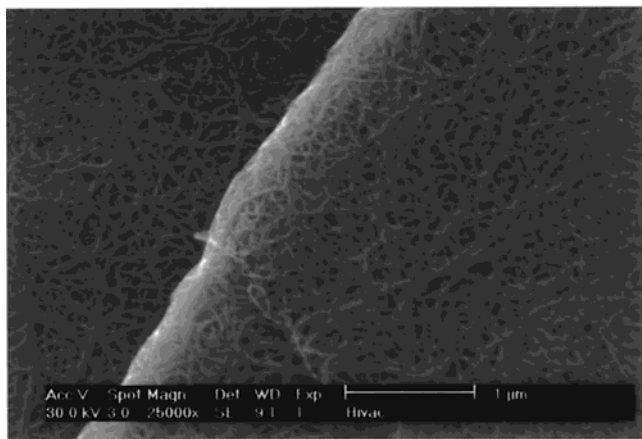


Figure 2. SEM image of carbon nanotubes produced by high-pressure CO decomposition (HiPco).

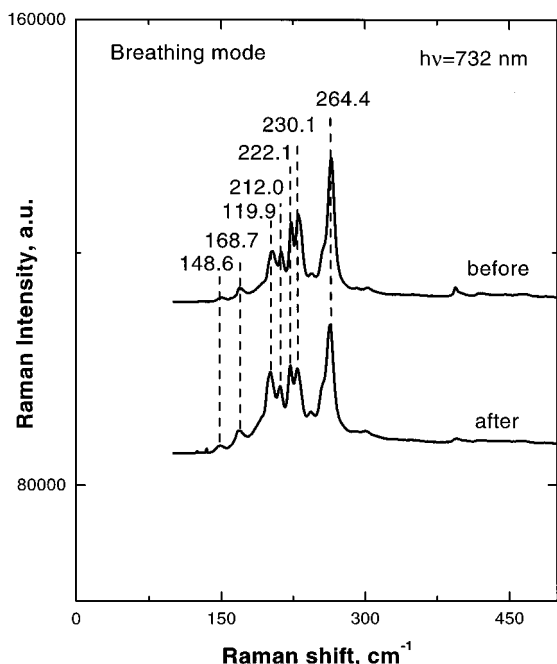


Figure 3. Raman spectra of HiPco nanotubes before and after NEXAFS experiment.

photons during the NEXAFS experiment or due to a thermally driven process, the SEM images of the samples deposited onto the Au-covered Ta foil were also measured after the NEXAFS experiment. The SEM images after the NEXAFS experiment showed an intact tubular structure, indicating that little or no degradation occurred.

Raman spectra were also measured from nanotubes before and after the NEXAFS measurements. The characteristic Raman active breathing mode of the nanotubes⁷ remains unchanged after the NEXAFS experiment. As shown in Figure 3, only a small change in Raman mode intensities is observed. The laser light wavelength used was 732 nm.

C. Preparation of Reference Organic Compounds. The NEXAFS spectra of (a) 9-phenanthrol (Aldrich, 99%), (b) xanthene (Aldrich, 99%), (c) anthraquinone (Aldrich, 97%), and (d) 9-anthracenecarboxylic acid (Aldrich, 99%) were measured using the same energy resolution as for carbon nanotubes (0.35 eV for C K-edge). The solid powders of the organic compounds were pressed onto a tungsten grid in a spot of area of ~ 0.25 cm². The tungsten grid was spot-welded onto the stainless steel sample holder. The samples were outgassed for 3–4 h. The background pressure in the chamber was 3×10^{-8} Torr before the NEXAFS experiment.

D. NEXAFS Technique. C K-edge and O K-edge NEXAFS spectra were measured at the National Synchrotron Light Source (NSLS), at the Brookhaven National Laboratory (U1 beam line). Synchrotron

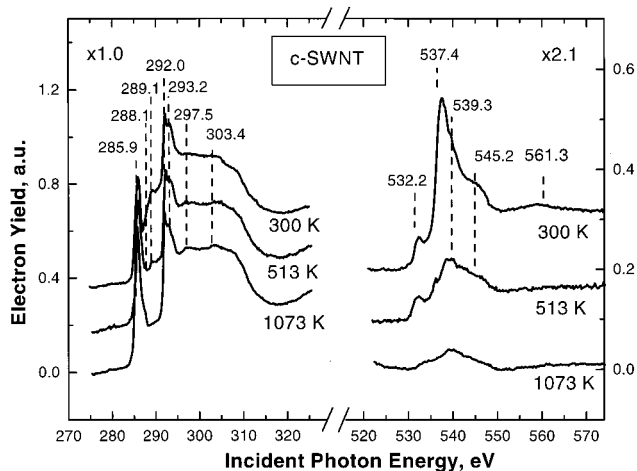


Figure 4. C K-edge and O K-edge NEXAFS of closed-end carbon nanotubes after heating to 300, 513, and 1073 K.

radiation was monochromatized with an SGM-type extended range grasshopper (ERG) monochromator. The setup has been described elsewhere.^{8,16} An ultrahigh vacuum (UHV) chamber is attached to the optical beam line through a UHV gate valve. The UHV chamber is equipped with an Auger spectrometer (Perkin-Elmer) and a UTI quadrupole mass spectrometer. Electron yield spectra are measured using a Channeltron multiplier located near the sample surface. A retarding potential of -100 eV at the entrance of the detector is used to repel low-energy electrons originating mainly from the bulk.

The NEXAFS spectra were obtained at the C K-edge energy region (from 275 to 325 eV). A few O K-edge region spectra were measured in the region from 521 to 591 eV, but these were less revealing in characterizing the surface functional groups on the nanotubes.

III. Results

A. NEXAFS of PLV Carbon Nanotubes. Figure 4 shows the C K-edge and O K-edge NEXAFS spectral region for c-SWNTs measured after thermal activation at 300, 513, and 1073 K. The C K-edge spectrum measured at 300 K is characterized by features at 285.9, 288.1, 289.1, 292.0, 293.2, 297.5, and 303.4 eV. Upon thermal treatment, all features in the spectrum increase in intensity except for those at 288.1 and 289.1 eV, which decrease in intensity significantly. The shoulder at 288.1 eV disappears after treatment at 513 K. The feature at 289.1 eV decreases mainly in the range 513–1073 K. The features at 288.1 and 289.1 eV are present as a result of oxygenated functionalities on the nanotubes and these functionalities decompose upon heating.

Figure 4 also shows O K-edge of NEXAFS spectra measured after 300, 513, and 1073 K treatment of the c-SWNT sample. The spectra are characterized at 300 K by features at 532.2, 537.4, 539.3, 545.2, and 561.3 eV. Upon heating from 300 to 1073 K, the features at 532.2, 545.2, and 561.3 eV decrease somewhat in intensity and the feature at 537.4 eV decreases significantly in intensity, revealing the feature at 539.3 eV.

A close similarity in the C K-edge and O K-edge region of the NEXAFS spectra for c-SWNT and o-SWNT samples is observed, comparing Figure 4 with Figure 5. C K-edge features are closely similar in energy (left-hand side of Figure 4 and left-hand side of Figure 5). A loss of intensity of the two features in the 288–290-eV range is observed for both c-SWNT and o-SWNT samples upon heating. The behavior of the O K-edge features for c-SWNT and the o-SWNT samples (right-hand side of Figure 4 and Figure 5) is also closely similar on heating.

B. NEXAFS of HiPco Carbon Nanotubes. Figure 6 shows the C K-edge and O K-edge spectra for the HiPco nanotube

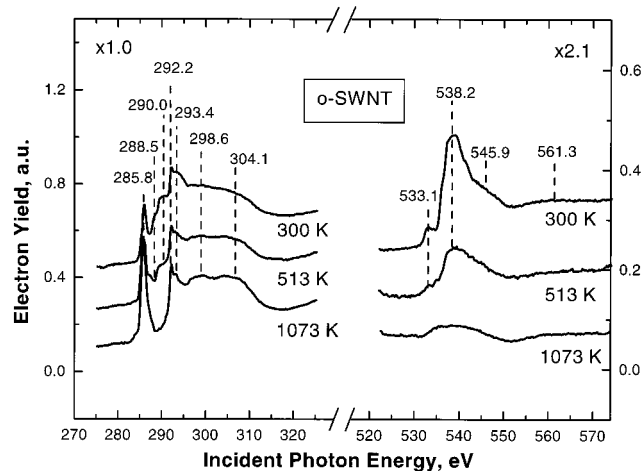


Figure 5. C K-edge and O K-edge NEXAFS of open-end carbon nanotubes after heating to 300, 513, and 1073 K.

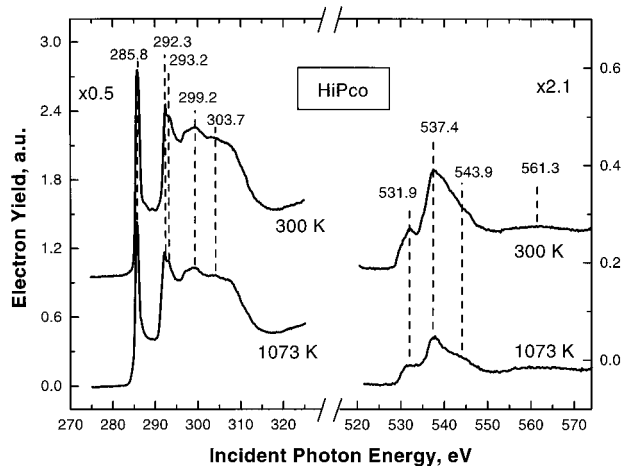


Figure 6. C K-edge and O K-edge NEXAFS of closed-end carbon nanotubes after heating to 300 and 1073 K. These nanotubes were made by the HiPco process and have not been treated by oxidizing acids.

sample at 300 K and following heating to 1073 K. The C K-edge spectra are very similar to those of c-SWNT and o-SWNT samples made by the PLV process with the exception of the features in the 289–292-eV range which are absent for HiPco material. Heating to 1073 K does not induce much change in either the line shape or relative intensities of the features in C K-edge spectrum in Figure 6.

The O K-edge spectra of the HiPco material (right-hand side of Figure 6) shows NEXAFS resonance energies similar to those for PLV tubes. Heating to 1073 K causes a decrease in intensities of all features, as is also seen for PLV material in Figure 4 and Figure 5.

C. NEXAFS of Reference Organic Compounds. C K-edge NEXAFS spectra of 9-phenanthrol, xanthene, anthraquinone, and 9-anthracenecarboxylic acid are shown in Figure 7. The assignments of NEXAFS resonances for the C K-edge spectra for all four compounds are summarized in Table 1.

Briefly, for these various fused-ring aromatic compounds, the C K-edge NEXAFS spectra are able to discriminate $\pi^*(\text{ring})$, $\pi^*(\text{C}=\text{O})$, $\sigma^*(\text{C}-\text{O})$, and $\sigma^*(\text{ring})$ features as shown in Table 1. The assigned modes on this basis will be useful in identifying the oxidized functionalities of the SWNT samples. In addition to our measurements, results from relevant previous studies support the assignments made in Table 1. In particular, for 9-anthracenecarboxylic acid, the $\pi^*(\text{ring})$ resonances are split by 1.6 eV in the work of ref 20, as we also find. Also, from the

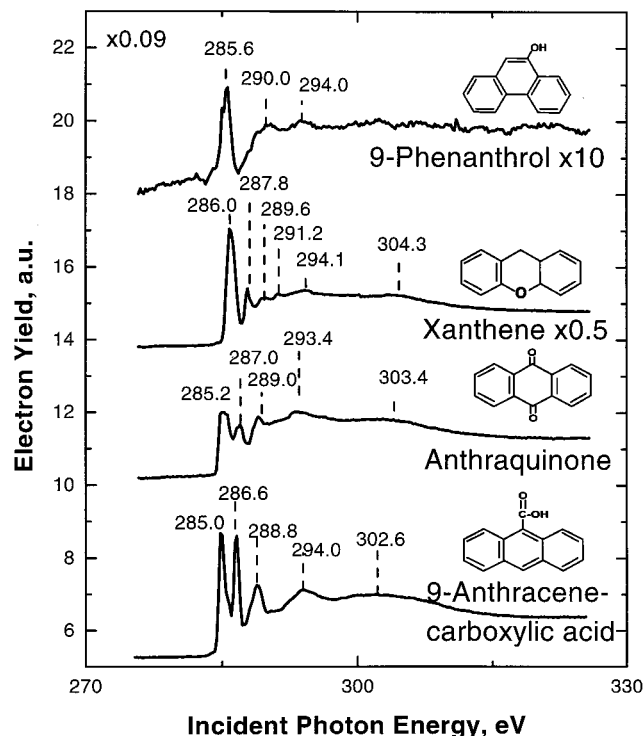


Figure 7. C K-edge NEXAFS of 9-phenanthrol, xanthene, anthraquinone, and 9-anthracenecarboxylic acid solids.

literature, the $\pi^*(\text{C}=\text{O})$ resonances at 288.8 eV was observed for acrylic acid²¹ and for propionic acid.²² For formic acid, the $\pi^*(\text{C}=\text{O})$ resonance is at 288.6 eV,²³ and for benzoic acid at 288.2 eV.²⁴ The $\sigma^*(\text{C}=\text{O})$ resonances occur at higher energies; i.e., for propionic acid $\sigma^*(\text{C}=\text{O})$ is at 302.5 eV²¹ and for acrylic acid the $\sigma^*(\text{C}=\text{O})$ resonance is at 304.0 eV.²¹ Further correlation with the literature can be found in references.^{20–30}

To confirm the assignment of the C K-edge features, we have also performed NEXAFS measurements at the O K-edge regions of the model compounds. However, because the compounds were pressed onto tungsten grids, containing a natural tungsten oxide film, the interference from O K-edge features of the substrate oxide prevents us from making a conclusive assignment in the O K-edge region.

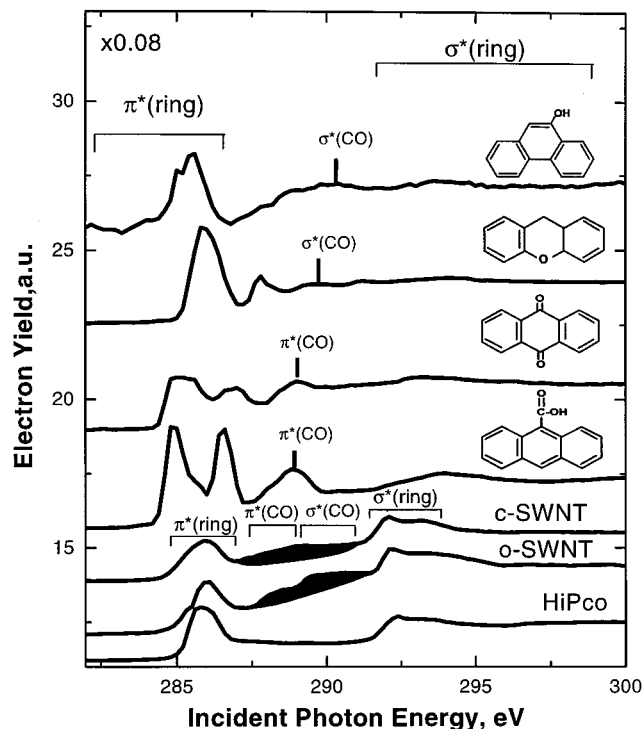
IV. Discussion

A. C K-Edge NEXAFS Spectral Assignments and the Thermal Stability of the Oxygen-Containing Functional Groups on SWNTs. Figure 8 shows a comparison of the C K-edge NEXAFS results on the three samples of SWNTs with

- (20) Ågren, H.; Vahtras, O.; Carravetta, V. *Chem. Phys.* **1995**, *196*, 47.
- (21) Bournel, F.; Laffon, C.; Parent, Ph.; Tourillon, G. *Surf. Sci.* **1996**, *352*, 228.
- (22) Bournel, F.; Laffon, C.; Parent, Ph.; Tourillon, G. *Surf. Sci.* **1996**, *350*, 60.
- (23) Ikeura-Sekiguchi, H.; Sekiguchi, T. *Surf. Sci.* **1999**, *433*, 549.
- (24) Bitzer, T.; Richardson, N. V.; Reiss, S.; Wühn, M.; Wöll, Ch. *Surf. Sci.* **2000**, *458*, 173.
- (25) Hasselström, J.; Karis, O.; Weinelt, M.; Wassdahl, N.; Nilsson, A.; Nyberg, M.; Pettersson, L. G. M.; Samant, M. G.; Stöhr, J. *Surf. Sci.* **1998**, *407*, 221.
- (26) Solomon, J. L.; Madix, R. J.; Stöhr, J. *Surf. Sci.* **1991**, *255*, 12.
- (27) Solomon, J. L.; Jordan-Sweet, J. L.; Kovac, C. A.; Goldberg, M. J.; Morar, J. F. *J. Chem. Phys.* **1988**, *89*, 2482.
- (28) Solomon, J. L.; Madix, R. J.; Stöhr, J. *J. Chem. Phys.* **1991**, *94*, 4012.
- (29) Nyberg, M.; Hasselström, J.; Karis, O.; Wassdahl, N.; Weinelt, M.; Nilsson, A.; Pettersson, L. G. M. *J. Chem. Phys.* **2000**, *112*, 5420.
- (30) Plashkevych, O.; Yang, L.; Vahtras, O.; Ågren, H.; Pettersson, L. G. M. *Chem. Phys.* **1997**, *222*, 125.

Table 1. NEXAFS C K-edge of Organic Compounds

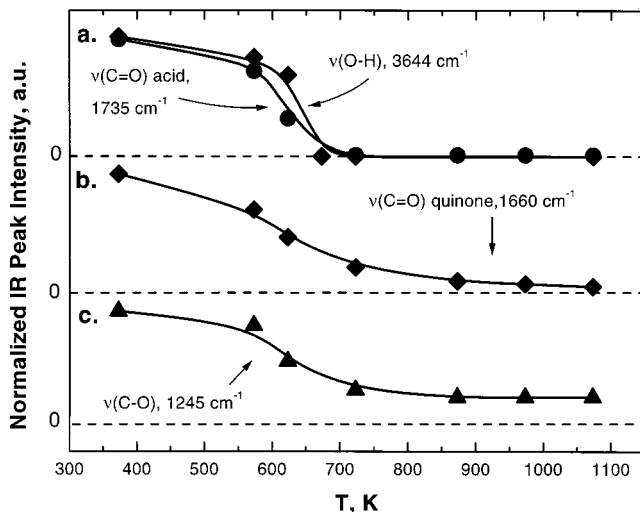
	<i>E</i> , eV	assignt	<i>E</i> , eV	assignt	<i>E</i> , eV	assignt	<i>E</i> , eV	assignt	<i>E</i> , eV	assignt
9-anthracene-carboxylic acid	285.0	$\pi^*(\text{ring})$	286.6	$\pi^*(\text{ring})$	288.8	$\pi^*(\text{C=O})$	294.0	$\sigma^*(\text{ring})$	302.6	$\sigma^*(\text{ring})$
anthraquinone	285.2	$\pi^*(\text{ring})$	287.0	$\pi^*(\text{ring})$	289.0	$\pi^*(\text{C=O})$	293.4	$\sigma^*(\text{ring})$	303.4	$\sigma^*(\text{ring})$
xanthene	286.0	$\pi^*(\text{ring})$	287.8	$\pi^*(\text{ring})$	289.6,	$\pi^*(\text{ring}) +$	294.1	$\sigma^*(\text{ring})$	304.3	$\sigma^*(\text{ring})$
					291.2	$\sigma^*(\text{C-O})$				
9-phenanthrol	285.6	$\pi^*(\text{ring})$			290.0	$\sigma^*(\text{C-O})$	294.0	$\sigma^*(\text{ring})$	302.5	$\sigma^*(\text{ring})$

**Figure 8.** C K-edge spectra of closed-end carbon nanotubes, open-end carbon nanotubes, HiPco nanotubes, and reference organic compounds (9-phenanthrol, xanthene, anthraquinone, and 9-anthracene-carboxylic acid).

the spectra measured for the standard compounds studied here. The $\pi^*(\text{ring})$ transitions are indicated in the range from about 285 to 287 eV; the $\sigma^*(\text{ring})$ transitions are in the range from about 292 to 294 eV. The oxidized carbon group resonances occur in the shaded sections of the nanotube spectra with $\pi^*(\text{CO})$ in the approximate range 287–289 eV and $\sigma^*(\text{CO})$ in the approximate range 289–291 eV. We focus our attention on the carbonyl resonances, which are found on both types of SWNTs that have been treated in oxidizing acids. These carbonyl resonances are not found on the HiPco material. It may be noted that, after removal of the oxygenated functional groups (darkened regions), the C K-edge NEXAFS spectra of the PLV SWNTs become very similar to the spectra of the HiPco SWNTs in Figure 8.

Resonances due to $\sigma^*(\text{C-H})$ bond generally have relatively low intensity and are often poorly resolved. They occur at energies close to those for $\sigma^*(\text{C-O})$ and largely overlap the latter. On the basis of the line shape of the resonance peaks and absence of C–H vibrational modes in the IR spectrum,² we assume that the $\sigma^*(\text{C-H})$ resonance is negligible in the NEXAFS spectra for the nanotube samples.

The thermal decomposition of the carbonyl-containing functional groups seems to occur first (the $\pi^*(\text{CO})$ features) (Figures 4 and 5), followed by the disappearance of the $\sigma^*(\text{CO})$ features associated with C–O single bonds. This suggests that single-bonded C–O–C species, such as ether-type species, may be

**Figure 9.** Temperature dependence of intensities of characteristic infrared spectral features observed during thermal decomposition.

more thermally stable than species containing π^* carbonyl orbitals. This observation is in accordance with infrared studies of the thermal stability of the functional groups, to be discussed below.

B. Infrared Studies of the Oxygen-Containing Functional Groups on SWNTs. The results in Figure 9 summarize the thermal behavior observed by IR spectroscopy for the acid-treated SWNTs.² It may be seen that the loss of –OH intensity and acid C=O intensity is closely correlated, indicating that these vibrational modes are derived from COOH groups on the nanotubes. They disappear together at temperatures below ~650 K. Quinone and ether groups have a higher temperature stability and show residual intensity in the infrared even after being heated to 1073 K. These general observations from infrared spectroscopic measurements are therefore in accord with the NEXAFS measurements where $\pi^*(\text{C=O})$ features disappeared first upon heating, followed by the disappearance of $\sigma^*(\text{CO})$ spectral features. The temperature scales in the NEXAFS measurements and in the IR measurements are not exactly comparable. For the IR measurements, the temperature scan rate was 3.8 K/s whereas for the NEXAFS measurements it was 1.0 K/s. Thus, for the IR measurements, changes will appear to occur at slightly higher temperatures than in the NEXAFS measurements.

C. Measurements of the Degree of Oxidation of the Nanotubes. As mentioned before, the oxygenated groups responsible for $\pi^*(\text{CO})$ and $\sigma^*(\text{CO})$ resonances in the C K-edge NEXAFS (287–291) eV region disappear upon heating and the C K-edge spectrum of PLV tubes becomes closely similar to that of the HiPco tubes (Figure 8). Differences in spectra for PLV and HiPco tubes are also observed in the O K-edge region at 300 K. In NEXAFS measurements, the height of the edge jump is related to the concentration of the element.⁸ For example, the edge jump for the C K-edge spectrum in the current study is defined as the intensity difference at energies before

Table 2. Relative Atomic Ratio of Oxygen Measured by Edge-Jump Method

carbon nanotubes	$(I_{\text{O}}/I_{\text{C}})(S_{\text{C}}/S_{\text{O}})$ (%) ^a		
	heated to 300 K	heated to 513 K	heated to 1073 K
c-SWNT	5.5	3.4	0.5
o-SWNT	6.7	4.2	0.7
HiPco	1.9		0.9

^a Calibration value measured by conversion of oxygenated functional groups to measured partial pressure of CO and CO₂ by heating.

the onset of C K-edge measurements (280 eV) and after the transitions (317 eV). The atomic ratio of oxygen atoms to carbon atoms, measured using the edge-jump technique⁸ is summarized in Table 2. The O/C atomic ratio for c-SWNT (300 K) was normalized to that measured by conversion of the oxygenated functional groups to measured partial pressures of CO and CO₂ by heating, which is determined to be 5.5%.^{6b} The O/C ratios for other samples and temperatures were estimated based on the normalized value for c-SWNTs. The quantities of oxide present on the oxidized tungsten grid will not change upon heating to 1073 K.³¹

Both o-SWNT and c-SWNT tubes have a similar oxygen/carbon atomic ratio (5.5–6.7%) at 300 K. The HiPco tubes have a lower oxygen atomic ratio (O/C = 1.9%) which agrees with the absence of observable π^* and $\sigma^*(\text{CO})$ resonances at 287–291 eV in the C K-edge NEXAFS spectra. When the nanotubes are heated to 1073 K, the atomic ratio of oxygen for each sample of carbon nanotubes decreases to ~1%. The O/C ratio of ~1% is comparable to a ratio of 3% measured earlier by Auger spectroscopy on the o-SWNTs after heating to 1073 K.⁵

V. Summary

The following conclusions have been made based on the C K-edge and O K-edge NEXAFS study of single-wall carbon nanotubes:

1. The presence of oxygen-containing functional groups is observed in C K-edge and O K-edge NEXAFS spectra of c-SWNTs produced by the PLV method and purified in oxidizing acidic solution.

2. Acid treatment of c-SWNTs using HNO₃/H₂SO₄ and acid cutting of c-SWNT using H₂O₂/H₂SO₄ both lead to SWNT material that exhibits similar $\pi^*(\text{CO})$ and $\sigma^*(\text{CO})$ C K-edge

(31) King, D. A.; Madey, T. E.; Yates, J. T., Jr. *J. Chem. Phys.* **1971**, *55*, 3247.

resonance energies, indicating a similar distribution of C=O and C–O–C groups.

3. The C K-edge resonances due to C=O-containing functional group ($\pi^*(\text{CO})$) disappear upon heating to ~513 K, whereas C–O functional groups disappear primarily in the range 513–1073 K.

4. Upon removal of oxidized functional groups by heating to 1073 K, the NEXAFS spectra of PLV nanotubes become similar to that of HiPco tubes that have not been oxidized in acidic media.

5. The O/C atomic ratio measured for HiPco tubes is much lower (1.9% O/C after 300 K) compared to O/C = 5.5–6.7% for PLV tubes that have been acid oxidized. After heating to 1073 K, the O/C ratio of both PLV and HiPco material decreases to ~1% as estimated by the NEXAFS edge-jump method.

6. A comparison has been made for the C K-edge for 9-phenanthrol, xanthene, anthraquinone, 9-anthracenecarboxylic acid, and carbon nanotube NEXAFS spectra. The nanotube resonance due to π^* transitions in the regions from 287 to 290 eV agrees with observed $\pi^*(\text{C}=\text{O})$ resonance of 9-anthracenecarboxylic acid (288.8 eV) and anthraquinone (289.0 eV); the NEXAFS nanotube resonances due to $\sigma^*(\text{C}-\text{O})$ for the acid-treated nanotubes from 290 to 291 eV agrees with the observed $\sigma^*(\text{C}-\text{O})$ resonance of 9-phenanthrol (290.0) and xanthene (289.6 eV).

7. Heating to remove the oxygenated functional group does not produce a significant change in the Raman spectra of the nanotube breathing modes, indicating that the tubular structure of the nanotubes is essentially preserved following the thermal degradation of the oxygenated functional groups of the surface.

8. These studies indicate that the oxygenated defect density on nanotube material that has been purified or cut in oxidizing acid media is very high. The O/C ratio measured indicates that oxygenated functional groups exist on the walls of acid-oxidized SWNTs at the 5–7% level.

Acknowledgment. We acknowledge the support of the Army Research Office (ARO) and of the Aberdeen Proving Grounds through ARO. We also acknowledge ExxonMobil for providing beam time at the U1A Beamline at Brookhaven National Laboratory. We also thank NSF for the financial support (Grant CTS-0074649).

JA011021B